Available online at www.sciencedirect.com

ScienceDirect

Physics Procedia 69 (2015) 320 – 326

Physics Procedia

10 World Conference on Neutron Radiography 5-10 October 2014

Edge Refraction Contrast Imaging on a Coventional Neutron Diffractometer Employing Dispersive Double-Crystal Monochromator

Pavol Mikula[a]*, Miroslav Vrána[a], Dušan Korytár[b]

[a]*Nuclear Physics Institute ASCR, v.v.i., 25068 Řež, Czech Republic*
[b]*Institute of Electrical Engineering, Slovak Academy of Sciences, Dúbravská cesta 9, 845 11 Bratislava, Slovak Republic*

Abstract

Slits and macroscopic objects such as edges give rise to interference effects when a coherent neutron (or X-ray) beam propagates through an investigated sample. These phenomena are effectively used in the so called phase-contrast imaging. In addition to the absorption contrast in the conventional radiography it exploits also these contributions from the induced phase shifts. However, the used radiation has to possess a sufficiently high spatial coherence. In this contribution we present a special neutron diffractometer performance (in two alternatives A and B) based on two bent perfect Si crystals which provides a high spatial coherence beam of sufficient intensity which could be potentially used in some phase contrast radiography experiments.

Selection and peer-review under responsibility of Paul Scherrer Institut

Keywords: Phase contrast; edge imaging; neutron diffraction; double-crystal monochromator

Introduction

Conventional radiography is based on absorption effects which depend only on the imaginary part of the refractive index. However, slits and macroscopic objects such as edges give rise to refraction and this phenomenon can be effectively used in the so called phase-contrast imaging. In addition to the absorption contrast in the conventional radiography it exploits also contributions of phase shifts induced by the propagation of a coherent

* Corresponding author. Tel.: +00420-266-173-159; fax: +00420-220-940-141.
E-mail address: mikula@ujf.cas.cz

Selection and peer-review under responsibility of Paul Scherrer Institut
doi:10.1016/j.phpro.2015.07.045

neutron (or X-ray) beam through an investigated sample as shown by e.g. Podurets et al. (1989), Allman et al. (2000), Thorton et al. (2003), Kardjilov et al. (2004), Lehmann et al. (2005) and Strobl et al. (2008, 2009). The difference in real part of the refractive index between a studied detail and its vicinity results in a phase shift between the wave transmitted through and outside the detail. Due to this phase shift, the two waves interfere. However, the used radiation has to possess a sufficiently high spatial coherence in order that one can detect the resulting interference pattern. The observation of the edge effects by using conventional double crystal diffractometer and their influence on radiography images have been first carried out with cold neutrons at the facility in BENSC in Berlin (see e.g. Treimer et al.(1996, 1998, 2005, 2011), Strobl et al. (2005) In this contribution we present properties of other neutron diffractometer performances based on two bent perfect Si crystals which provide a high spatial coherence of the thermal neutron beam (λ=0.162 nm) of sufficient intensity and beam cross-section which could be potentially exploited in some phase contrast imaging experiments.

2. Possible diffractometer settings providing a high spatial coherence

It is clear that a simple one crystal monochromator cannot provide the monochromatic beam with a high spatial coherence. It is brought about by the fact, that all individual points of the monochromator reflect divergent bunches

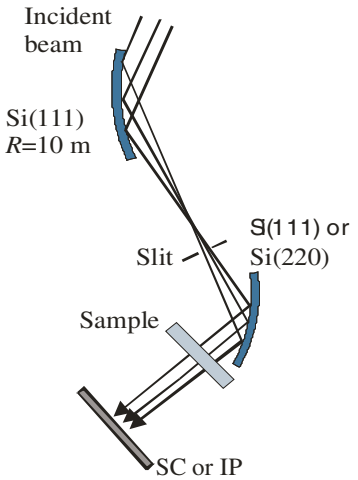

Fig. 1. Scheme of the diffractometer performance.

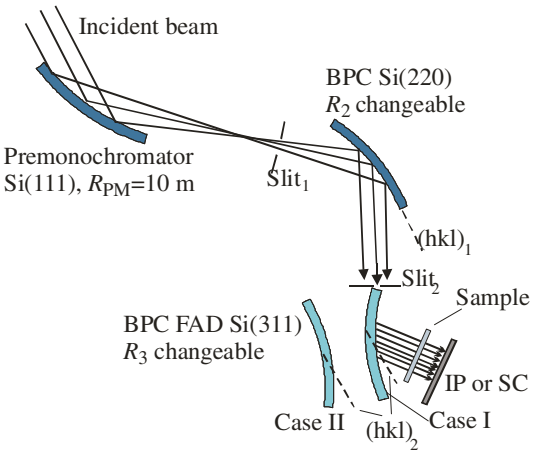

Fig. 2. Sketch of the experimental setting as used for the edge refraction contrast imaging studies where the BPC Si(311) FAD crystal was used in dispersive setting with respect to the Si(220) one.

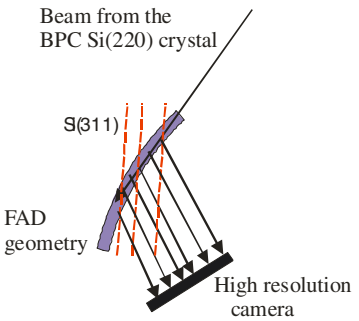

Fig. 3. Schematic sketch showing the detail of the FAD geometry of the Si crystal slab as used in the experiment.

of the rays which at some distance mutually mix. Moreover, if the monochromator crystal has its own characteristic mosaicity, the bunches from different points differ also in $\Delta\lambda$ spread because of the mosaic distribution. Remember that in the case of bent perfect crystal it is so called effective mosaicity according to Mikula et al. (2004). The decrease of the divergence by using Soller collimators to achieve a required spatial coherence becomes inpracticable because it would result in a significant decrease of the instrument luminosity due to a rather high number and absorption of the Soller collimator sheets.

However, the beam collimation without using the Soller collimator can be substantially improved by using a double-crystal monochromator system when both crystals are mutually in dispersive or quasi-dispersive setting. If we avoid the case of flat perfect crystals providing in the dispersive setting an extremely high resolution but low luminosity (see

e.g. Bacon, 1975), it is valid also in the case of the employment of bent perfect crystals in the so called parallel (1,-1) setting. It is well known, that the (1,-1) setting of the same crystal slabs (in our case Si(111) slabs), is fully nondispersive only in the case of flat perfect crystals. But in the case of bent perfect crystals due to a nonnegligible divergence of the beam reflected by the first crystal as well as its thickness, the second bent crystal situated at some distance from the first one cannot collect and diffract all neutrons impinging on it (as it is in the case of flat crystals), because the divergent neutrons meet on the second bent crystal a slightly different Bragg condition. This effect takes place for any curvature of the second crystal and becomes stronger with increasing the distance between the crystals. Also, double-crystal rocking curves become wider (see Figs. 4 and 5). On the other hand, it improves considerably the collimation of the double reflected beam and simultaneously, monochromatic neutron current correspondingly decreases.

Another possibility of decreasing the divergence of the double reflected beam is the use of dispersive setting of two crystals of different orientations. If they are employed in symmetric reflection geometry, the double reflected beam is narrow and not suitable for radiographic experiments. However, if the second crystal is in fully asymmetric diffraction (FAD) geometry (see Figs. 2 and 3) the beam coming from the first crystal is in the second one spread along its longest edge (due to a low attenuation factor silicon is a very suitable material). Then, the double reflected beam can be wide of several centimetres and locally one can achieve a good spatial coherence.

3. Experimental results

3.1. (1,-1) diffraction performance with the 2 mm thick Si(111) second slab

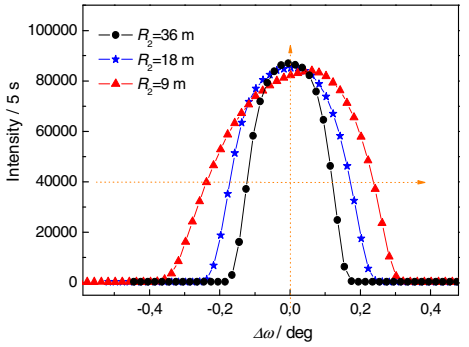

Fig. 4. Rocking curves of the Si(111) bent crystal of t=2 mm (different R_2) with respect to Si(111) of t=4 mm (fixed R_1=12 m) in the parallel (1,-1) setting.

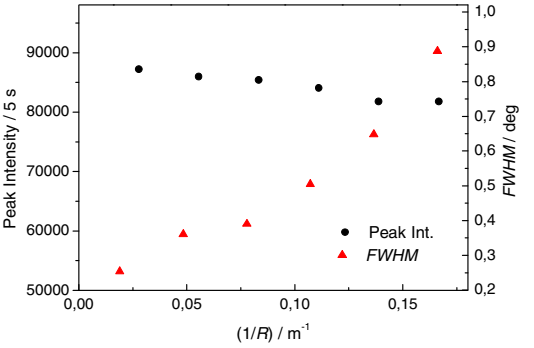

Fig. 5. The dependences of the peak intensity and FWHM of the rocking curves on the curvature of the second crystal of the parallel DC (1,-1) setting.

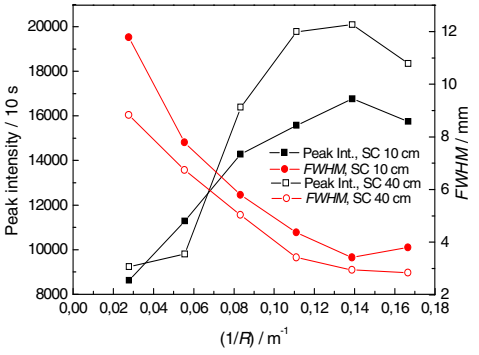

Fig. 6. Parameters of the diffraction profiles registered by a scintillation camera SC at the distance of 10 cm and 40 cm from the sandwich

The diffraction profiles registered by a scintillation camera (SC) having the spatial resolution of 0.1 mm for two distances of 10 cm and 40 cm from the second crystal are shown in Fig. 6. It can be seen from Fig. 6 that *FWHM* of the beam profile decreases and the peak intensity increases (up to a saturation) with the increase of the curvature. It is mainly brought about by increasing the effective mosaicity of the second crystal. However, when comparing the *FWHM* dependences corresponding to the distances of 10 cm and 40 cm, it can be seen that there is only a small focusing effect slightly dependent on the curvature. High resolution properties of the monochromatic beam are then documented in the following Figs. 7 and 8, where edge profiles obtained on several samples are shown.

The samples were installed behind the second crystal and the imaging plate (IP) with the spatial resolution of 50 μm was put at the distance of 50 cm from the samples. Inspection of Fig. 8 reveals that in the case of imaging on the group of office staples the related maxima and minima from individual staples (of the group) partly overlap and therefore, the phase contrast is much smaller in comparison with the individual office staple, or at the end of the group of them.

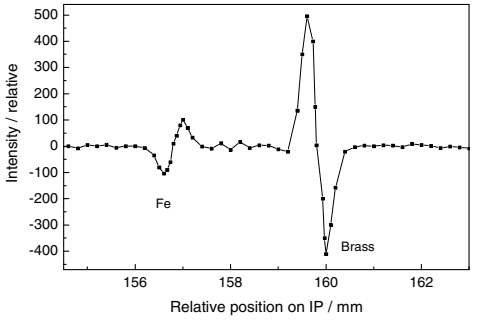

Fig. 7. Experimental profiles obtained on 2 mm Fe and 19 mm brass edges registered by means of the imaging plate (IP).

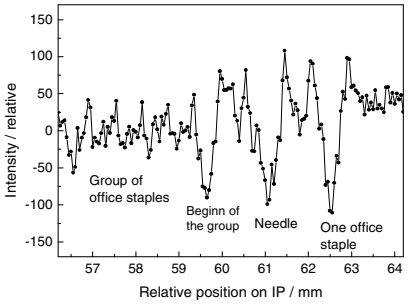

Fig. 8. Edge profiles obtained on mutually separated one office staple, hypodermic needle and a group of the staples.

3.2. (n,-m) diffraction performance with the 3 mm thick Si(220) second slab

If different crystal cuts are used in the parallel double-crystal setting, we could expect that such setting is much more dispersive and the double diffracted beam should be less divergent and correspondingly less luminous. However, Fig. 9 documents that in this case, the *FWHM* of the rocking curve is narower than in the case of the bent Si(111) crystal (see Fig. 5) and on the other hand, the beam profiles shown in Fig. 10 are wider (compare with Fig. 6). Also in this case the real space focusing is very small. It means that with the curvature of the second crystal one can easily manipulate the dispersity of the double-crystal setting. In our case, it resulted from the experimetal arrangement (see Fig. 1) in a fact that the combination of curved crystals Si(111)+Si(220) is less dispersive than Si(111)+Si(111). Nevertheless, the double reflected beam still has excellent parameters concerning the luminosity and the collimation and can be used for phase contrast imaging. Figs. 11 to 13 show experimental examples of the edge profiles obtained on the faces of rather thick rectangular samples for two different radii of curvatures of the Si(220) crystal. It can be seen that the imaging contrast depends on the material (on the coherent scattering amplitude of neutron) as well as its edge width. In all cases the time for taking the edge images on IP was approximately 10 hours. In principle, the contrast is better for smaller curvature of the Si(220) crystal slab, however, the time for imaging is shorter for larger curvatures. Moreover, the cross-section of the beam is much

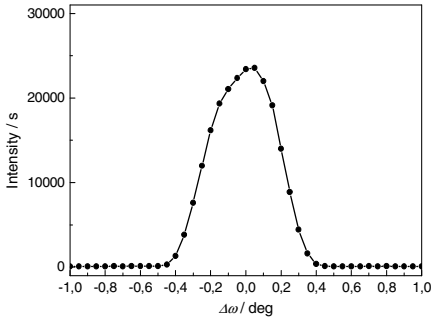

Fig. 9. Example of the DC rocking curves Si(220) crystal (t=3 mm) with respect to the Si(111) one for the curvature of 0.167 m^{-1} (R_2=6 m) .

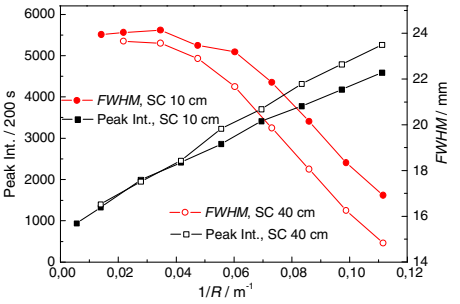

Fig. 10. Beam profiles measured by means of SC situated at the distance of 10 cm and 40 cm from the Si(220) crystal for different of curvatures (1/ R_2).

smaller for larger curvatures.

3.3. Three axis Si(111)+(n,-m,) diffraction performance with the third FAD crystal slab

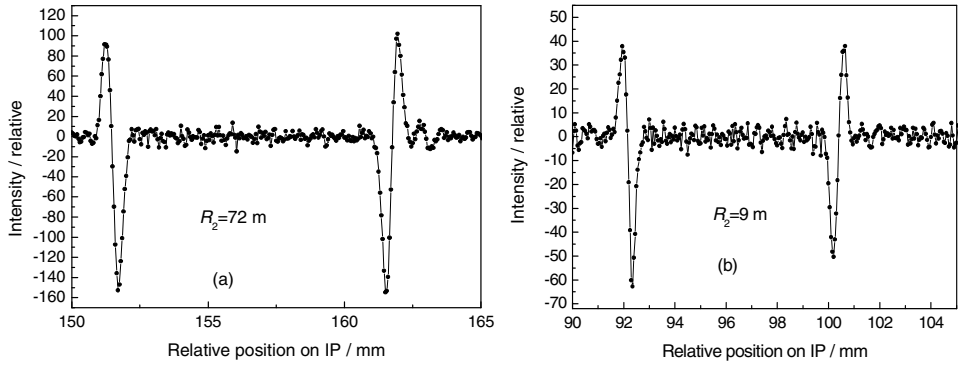

Fig. 11. Experimental edge profiles obtained on both sides of squared 9 mm α-Fe prism and registered by IP at 40 cm from the sample and for R_2=72 m (a) and R_2=9 m (b).

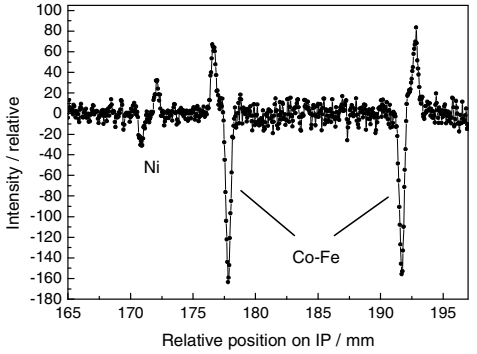

Fig. 12. Experimental edge profiles obtained on the two sides of a Co-Fe plate and a Ni sample both of the thickness of 3 mm for R_2=8 m.

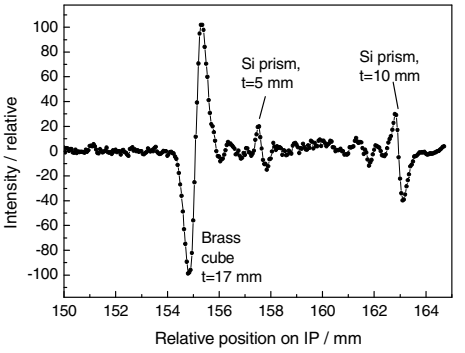

Fig. 13. Edge profiles obtained on three samples with different widths of the edges and registered by IP at 40 cm from the sample for R_2=9 m.

In this case, the bent Si(111) crystal, due to its large lattice constant, can be considered as premonochromator for the next double crystal (n,-m) aranngement when providing rather divergent monochromatic beam of a large $\Delta\lambda$ spread (see Fig. 2). Even though the beam after the diffraction on the bent Si(220) crystal is well prepared for refraction edge imaging, by using a third crystal slab in FAD geometry it can be further manipulated with the beam cross-section and beam collimation. First, the geometry - marked as case I (see Fig. 2) - of the FAD crystal was

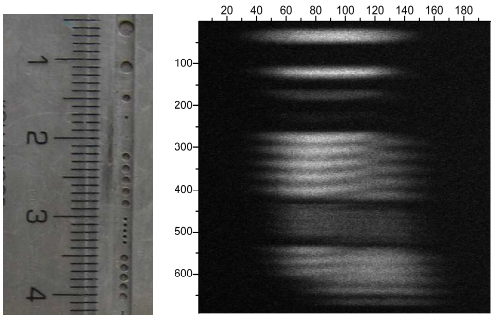

Fig. 14. (a) The holes in the Cd absorber situated vertically in front of the FAD crystal and (b) the image of them for R_2 = 36 m and R_{FAD} = 9 m. IP was at 10 cm from the FAD crystal. The numbers on the x and y axes are the pixel numbers. Case I.

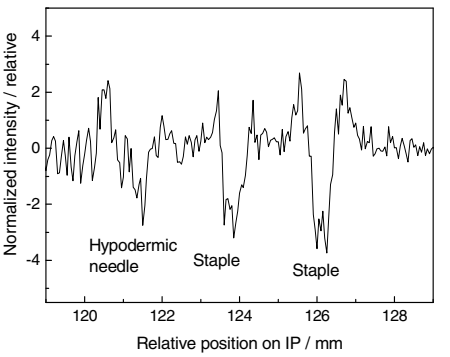

Fig. 15. Edge images from a hypodermic needle and two individual office staples: (a) with R_2 =36 m, R_3 = 36 m and the IP 38 cm from the sample. Case I.

tested. The effect of cross section manipulation is demonstrated in Fig. 14 by imaging vertically arranged small holes in a Cd sheet situated just before the front face of the FAD crystal in the place of slit S_2. It can be seen from Fig. 14 that the FAD crystal works as an one dimensional magnifier. For small curvatures of the FAD crystal the spreading of the beam inside of it can be several centimetres. The high resolution properties of the spread beam obtained by the FAD crystal are also demonstrated by the images of two office staples and a hypodermic needle (see Fig. 15) put just behind the FAD crystal. In the case of the office staples, the evidence of typical refraction at the sharp edges can be seen. However, there are no sharp edges in the case of the hypodermic needle and the corresponding image is blurred. Similarly to the case I, as shown in the following Figs. 16, 17 and 18, the refraction edge effects, however, with a better contrast, were observed also in the case II of the FAD geometry. Fig. 16 shows the refraction effect at the right blunt edge of the workshop knife (see the related photo). However, no refraction effect was seen on the imaging of the sharp left side of the knife, where there is no rectangular shaped edge but a wedge with a very thin end. Fig. 18 shows the images of the refraction at the edges of 5 mm thick stainless steel and steel plates put about 4 mm side by side. As the steel is magnetic, there is also some contribution to the refraction from the magnetic scattering amplitude, as can be seen from Fig. 18. The major maximum and minimum are slightly wider than the ones corresponding to the stainless steel sample.

4. Conclusion

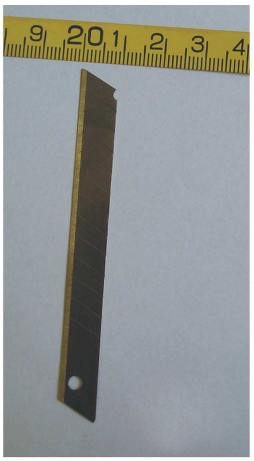

(*a*)

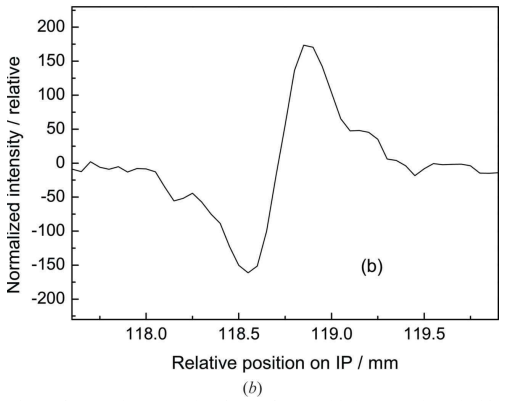

(*b*)

Fig. 16. (a) Photograph of a 0.5 mm thick workshop knife and (b) the intensity profile related to edge image in the vicinity of the right-hand blunt edge. Case II.

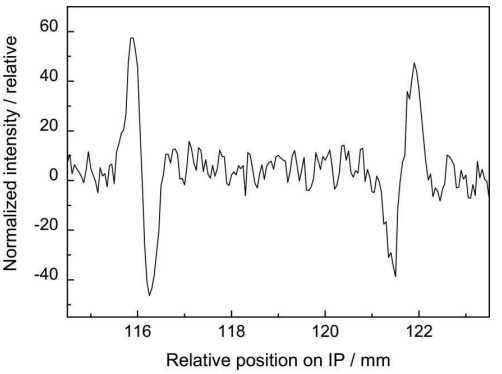

Fig. 17. Intensity profiles related to imaging of the 10 mm wide edges of a rectangular Si rod of cross-section 5x10 mm. Case II.

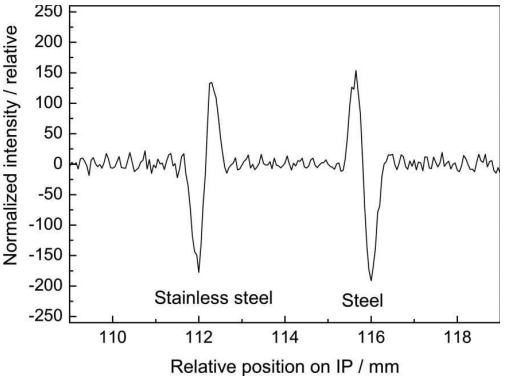

Fig. 18. Intensity profiles related to imaging in the vicinity of the edges of 5 mm thick stainless steel and steel plates. Case II.

The quasi-dispersive double bent crystal setting provides a highly parallel monochromatic beam having cross-section of several square centimeters which can be used, besides other things, for radiography experiments. Moreover, the beam possesses a sufficiently high spatial coherence and thus, it can be used for studies of the phase shift contrast phenomena. As can be seen from Figs. 11 and 12, the edge profiles can be observed in a large range of the crystal curvatures of the Si(220) crystal which give the possibility to make a required time for imaging shorter. Further more, it is clear from Figs. 11 to 13 that the contrast of the profile depends on the thickness of the material as well as on the value of the coherent scattering length. A big difference in the contrast between Ni and Co-Fe samples (see Fig. 12) points out on a strong magnetic contribution for the latter one. However, it should be pointed out that the experimental performance has such excellent properties only in one dimension, i.e. in the scattering plane. As demonstrated in Fig. 14 the spatial coherence and quasi-magnifying property can be in some range easily manipulated by changing the curvature of the FAD crystal. However, this magnifying property has a limited utilisation when the signal related to an inhomogeneity is smeared along the longest edge of the FAD crystal without special effect on the resolution of its details. Finally, it should be also mentioned that a high spatial coherence beam can be also obtained by the realisation of a double reflection process inside one bent crystal which is generally called multiple reflection process. As indicated by Mikula et al. (2013), the multiple reflection provides a better spacial coherence beam, but one pays for it by by about one order of magnitude lower luminosity.

Acknowledgements

The measurements were carried out at the CANAM infrastructure of the NPI ASCR Rez. Bragg diffraction optics investigations are in the Czech Republic supported by the ESS project LM2010011: ‘Contribution to Partnership in Large Research Infrastructure of Pan-European Importance’ as well as by the project of EU-FP7-NMI3 II: “Integrated Infrastructure Initiative for Neutron Scattering and Muon Spectroscopy”, 2009-2015.

References

Allman, B.E., McMahon, P.J., Nugent, K.A., Paganin, D., Jacobson, D.L., Arif, M., 2000. Imaging: Phase Radiography with Neutrons. Nature, 408, 158-159.

Bacon, G. E., 1975. Neutron Diffraction, Oxford: Clarendon Press.

Kardjilov, N., Lehmann, E., Steichele, E., Vontobel, P., 2004. Phase-Contrast Radiography with a Polychromatic Neutron Beam. Nucl. Instrum. Methods in Phys. Res. A 527, 519-530.

Lehmann, E., Lorenz, K., Steichele, E., Vontobel., P. 2005. Non-destructive Testing with Neutron Phase Contrast Imaging, Nucl. Instrum. Methods in Phys. Res. A 542, 95-99.

Mikula, P., Kulda, J., Vrána, M., Chalupa, B., 1984. A Proposal of a Highly Efficient Double Crystal Monochromator for Thermal Neutrons. J. Appl. Cryst. 17, 189-195.

Mikula, P., Vrána, M., Šaroun, J., Krejčí, F., Seong, B.S., Woo, C., Furusaka, M., 2013. Some Properties of the Neutron Monochromatic Beams Obtained by Multiple Bragg Reflections Realized in Bent Perfect Single Crystals. J. Appl. Cryst. 46, Part 2, 128-134.

Podurets, K.M., Somenkov, e.a., Chistyakov, R.R., Shilstein, S.Sh., 1989. Visualisation of Internal Domain Structure of Silicon Iron Crystals by Using Neutron Radiography with Refraction Contrast, Physica B: Condensed Matter, 156-157, 694-697.

Strobl, M., Treimer, W., Kardjilov, N., Hilger, A., 2005. Application of Refraction Contrast Tomography, Nucl. Instrum. Methods in Phys. Res. A 542, Issues 1-3, 383-386.

Strobl, M., Treimer, W., Kardjilov, N., Hilger, A., Zabler,S., 2008. On Neutron Phase Contrast Imaging, Nucl. Instrum. Methods in Phys. Res. B 266, 181-186.

Strobl, M., Kardjilov, N., Hilger, A., Kune, G., Frei, G., Manke, I., 2009. High Resolution Investigation of Edge Effects in Neutron Imaging, Nucl. Instrum. Methods in Phys. Res. A 604, 640-645.

Thorton, J., McMahon, P.J., Allman, B.E., Murphy, J.E., Nugent, K.A., Jacobson, D.L., Arif, M., Werner, S.A., 2003. The Detection of Flaws in Components from the Hot-End of Gas Turbines Using Phase-Contrast Radiography with Neutrons: Feasibility Study. NDT&International 36, 289-295.

Treimer, W., Schaper, J., 1996. Investigation of Refraction of Cold Neutrons at Neutron Tomographies. BENSC Exp. Rep. p 321.

Treimer, W., Feye-Treimer, U., Herzig, C., 1998. On Neutron Tomography, Physica B 241-243 1197-1203.

Treimer, W, Hilger, A., W., Kardjilov, N., Strobl, M., 2005. Review about Old and New Imaging Signals for Neutron Computerized Tomography, Nucl. Instrum. Methods in Phys. Res. A 542, Issue 1-3, 367-375.

Treimer, W., Feye-Treimer, U., 2011. On Coherence in Neutron Imaging, Nucl. Instrum. Methods in Phys. Res. A 651, 117-120.